Hindawi

Research Article

Effects of Lycium Barbarum Polysaccharides on the Metabolism of Dendritic Cells: An *In Vitro* Study

Baochen Zhang [ID],[1] **Kengyu Chen** [ID],[1] **Li Liu** [ID],[1] **Xiuyun Li** [ID],[2] **Enhui Wu** [ID],[1] **Liang Han** [ID],[3] **Zhongfeng Shi** [ID],[2] **and Xiangliang Deng** [ID][1]

[1]School of Chinese Medicine, Guangdong Pharmaceutical University, Guangzhou, Guangzhou 510006, China
[2]School of Pharmacy (The Center for Drug Research and Development), Guangdong Pharmaceutical University, Guangzhou, Guangzhou 510006, China
[3]School of Health (Guangdong Light and Health Engineering R&D Center), Guangdong Pharmaceutical University, Guangzhou, Guangzhou 510006, China

Correspondence should be addressed to Zhongfeng Shi; 956551063@qq.com and Xiangliang Deng; gzy622@163.com

Targeting dendritic cells (DCs) metabolism-related pathways and in-situ activation of DCs have become a new trend in DC-based immunotherapy. Studies have shown that *Lycium barbarum* polysaccharide can promote DCs function. This study is aimed at exploring the mechanism of LBP affecting DCs function from the perspective of metabolomics. MTT method was used to detect the activity of DC2.4 cells. ELISA kit method was used to detect the contents of IL-6, IL-12, and TNF-α in the supernatant of cells. Ultra-performance liquid chromatography-quadrupole-time-of-flight mass spectrometry (UPLC-Q-TOF/ MS) was used to detect general changes in DC2.4 cell metabolism. And then multidistance covariates and bioinformatics, partial least squares-discriminant analysis (PLS-DA) were used to analyze differential metabolites. Finally, metabolic pathway analysis was performed by MetaboAnalyst v5.0. The results showed that LBP had no significant inhibitory effect on the activity of DC2.4 cells at the experimental dose of 50-200 μg/ml. LBP (100 μg/ml) could significantly stimulate DC2.4 cells to secrete IL-6, TNF-α, and IL-12. Moreover, 20 differential metabolites could be identified, including betaine, hypoxanthine, L-carnitine, 5'-methylthioadenosine, orotic acid, sphingomyelin, and L-glutamine. These metabolites were involved 28 metabolic pathways and the top 5 metabolic pathways were aspartate metabolism, pyrimidine metabolism, phenylacetate metabolism, methionine metabolism, and fatty acid metabolism. These results suggest that the effect of LBP on DCs function is related to the regulation of cell metabolism.

1. Introduction

Dendritic cells (DCs) were discovered and identified as highly effective antigen-presenting cells that can differentiate and capture antigens, before they migrate to the lymph node to present antigens and effectively activate T cells [1]. Currently, among the five types of DCs, conventional DCs (cDCs) including cDCs1 and cDCs2 can, respectively, polarize naive CD8^{+} and CD4^{+} T cells [2]. Also, DCs can induce cytotoxicity and proliferation of natural killer (NK) cells through direct cell-cell interaction and the secretion of some cytokines (e.g.,

IL-12, IL-15, etc.) [3]. The effects of DCs on the function of T cell and NK cell contribute to promoting the antitumor immunity. For example, when DCs recognize tumor antigens, they will be activated and migrate to the tumor draining lymph nodes to present tumor antigen information to T cells, in which T cells are then activated and differentiated into antitumor effector T cells [4]. Due to the influence of tumor microenvironment on DCs metabolism, DCs in tumor tissues are mostly immature [5]. Thus, targeting dendritic cells (DCs) metabolism-related pathways and in-situ activation of DCs have become a new trend in DC-based immunotherapy [6].
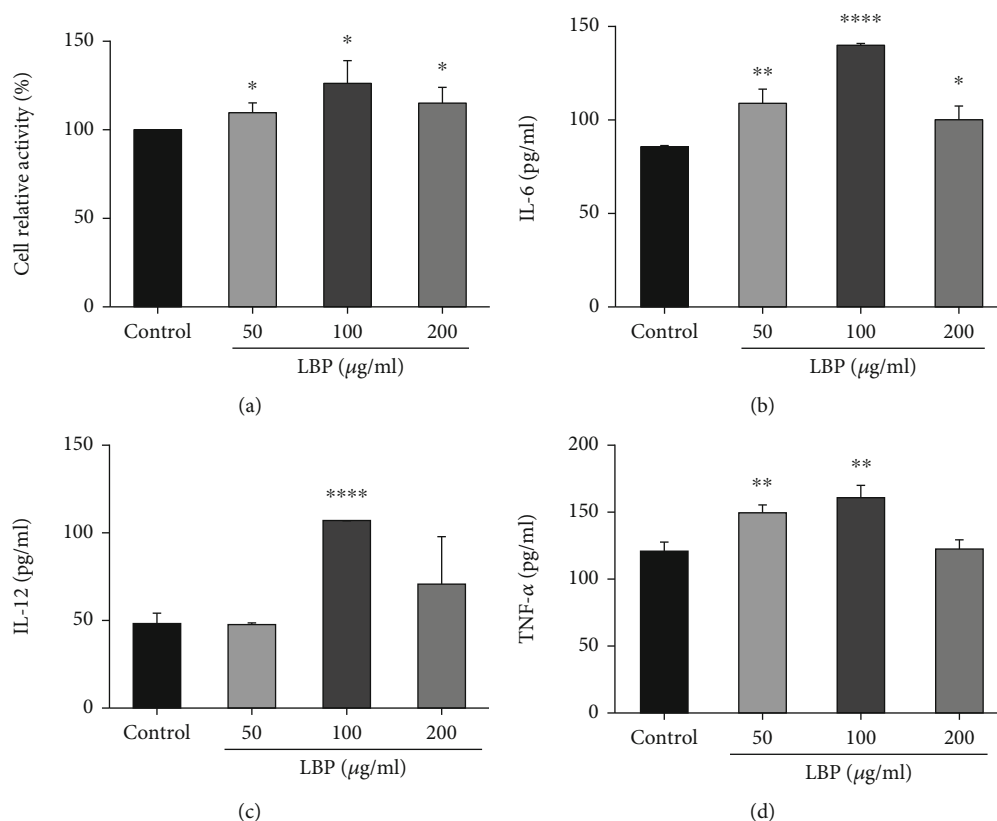
(a)

(b)

(c)

(d)

FIGURE 1: The effect of *Lycium barbarum* polysaccharide (LBP) on activity and cytokine production of DCs. (a) LBP had no significant inhibitory effect on DC2.4 cells. The cells were inoculated into 96-well plates and cultured in complete medium with different concentrations of LBP (0, 50,100, 200 μg/mL) for 24 h. (B-D) LBP induced the production of IL-6, IL-12, and TNF-α in DCs. ELISA kits were used to detect the levels of IL-6, IL-12, and TNF-α. Data were expressed as mean $\pm$ SD, $n = 3$ for each group. $^{*}P < 0.05$, $^{**}P < 0.01$, $^{****}P < 0.0001$ versus Control group.
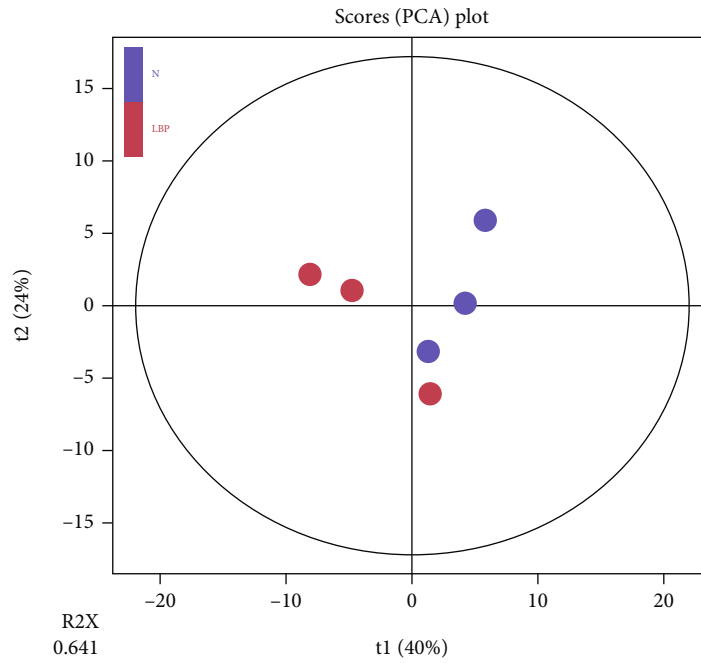
As traditional Chinese medicine, the fruits of *Lycium barbarum* are officially listed in the Chinese pharmacopeia. Polysaccharides are bioactive constituents of *Lycium barbarum* and have many biological activities, including antitumor and immunomodulatory effects. Promoting the functional maturation of dendritic cells is one of the important immunomodulatory effects of *Lycium barbarum* polysaccharides (LBP). Studies have indicated that LBP could promote the maturity of murine DCs maybe through TLR4-Erk1/2-Blimp1 and TLR2/TLR4-MyD88-NF-κB/p38 and Notch signaling [7–10]. Furthermore, LBP could strengthen DC mediated T lymphocyte cytotoxicity [10] and enhance the antitumor immune response in tumor-bearing mice [11]. However, it is not clear now which metabolic pathways are involved in the promotion of DCs maturation by LBP.

Based on the complexity of the multitarget and multipathway of traditional Chinese medicine, traditional research methods and analysis techniques are not enough to explain the specific mechanism of the detected biomarkers. Metabolomics as a cutting-edge analysis technology is widely used in the pharmacological research of traditional Chinese medicine by detecting and screening out statistically significant metabolites from biological samples [12]. In this way, metabolomics was used to investigate the effects of *Lycium barbarum* polysaccharides on the metabolism of dendritic cells in the present study.

2. Materials and Methods

2.1. Reagents. LBP, also named LBP3, were prepared as be described in our previous study with molecular weights range from 40 kDa to 350 kDa and the level of lipopolysaccharide was under the detection limit [13, 14]. DMEM were obtained from Gibco (USA, Lot No. 8119929). PBS buffer 1× was purchased form Wuhan Boshide Biological Engineering Co., Ltd. (Wuhan, China, Lot No. 14I17B30). Fetal bovine Serum (FBS) was obtained from Biological Industries (Israel, Lot No. 1924622). Methanol (AR) was purchased from Shanghai Anpu Experimental Technology Co., Ltd. (Shanghai, China, Lot No. Z5400144). Acetonitrile (AR) was purchased from Shanghai Anpu Experimental Technology Co., Ltd. (Shanghai, China, Lot No. C3010432). Ammonium acetate (AR) was purchased from Tianjin Zhiyuan Chemical Reagent Co., Ltd. (Tianjin, China, Lot No. 201840182077). LK16-HF90 CO_2 Incubator was purchased from Beijing Zhongxin Huada Technology Co., Ltd. (Beijing, China).

Scores (PCA) plot

N

LBP

t2 (24%)

t1 (40%)

R2X
0.641

(a)

Scores (PLS-DA) plot

N

LBP

t2 (16%)

t1 (40%)

R2X	R2Y	Q2Y		RMSEE	pre
0.738	0.999	0.798		0.033	3
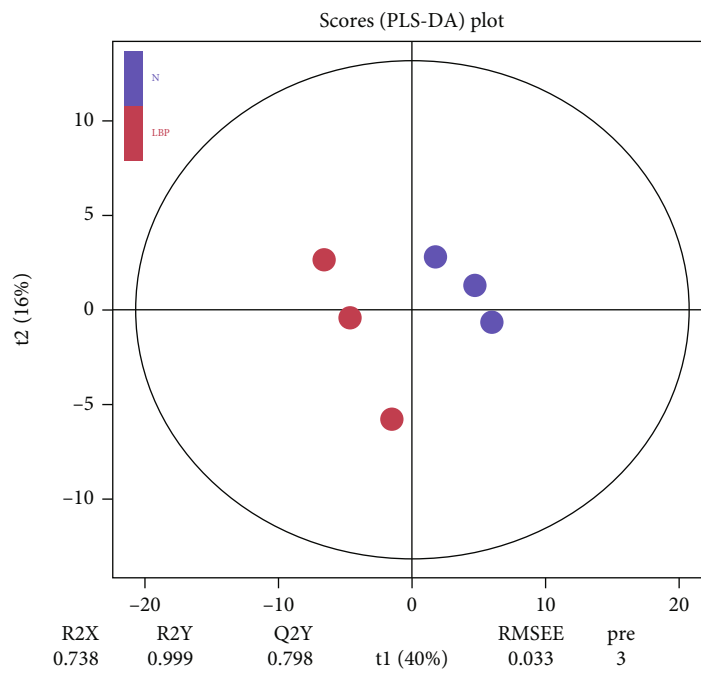
(b)

FIGURE 2: Continued.

(c)

(d)
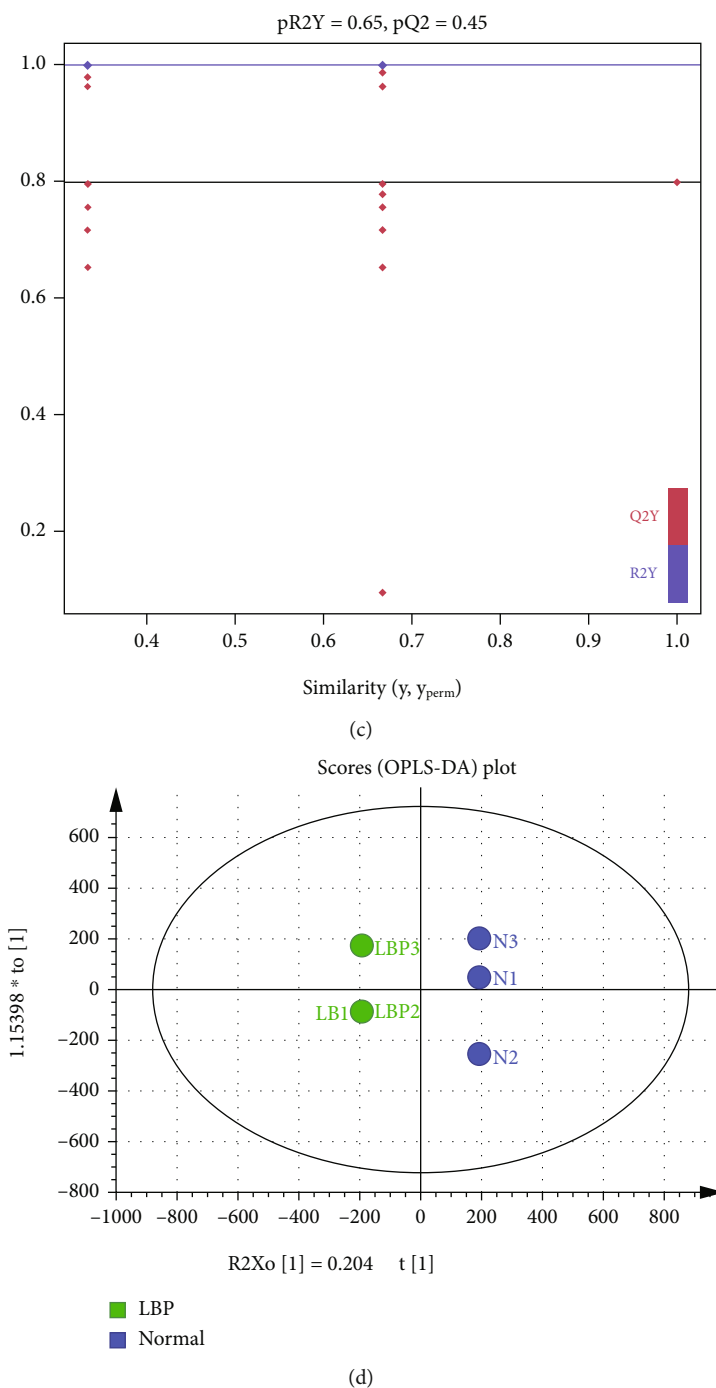
Figure 2: The scores plot of PCA, PLSDA and OPLS-DA. (a) PCA analysis. (b) PLS-DA model. (c) OPLS-DA score diagram and (d) load diagram.

SW-CF-2FD Ultra-clean table was purchased from Jiangsu Sujing Antai Co., Ltd. (Jiangsu, China). Fresco17 high speed refrigerated centrifuge was obtained from Thermo (USA). Pipettes were obtained from Thermo (USA, range 1000, 200, 100, 10 μL). DHP-9272 electronic analytical balance was purchased from Sartorius Scientific Instrument (Beijing) Co., LTD. (Beijing, China). Spectramax Plus 384-plus Microplate reader was obtained from MD (USA).

2.2. Cell Culture. Mouse bone marrow derived dendritic cell line DC2.4 was donated by Professor Zhou Lian of Guangzhou University of Chinese Medicine and purchased from Qingqi (Shanghai) Biotechnology Development Co., Ltd. (Shanghai, China). Cells were cultured in DMEM medium containing 10% FBS, 100 μg/mL streptomycin and 100 U/mL penicillin in a cell incubator where the condition is maintained at 37°C with 5% CO_2.

TABLE 1: Cell significantly different metabolites.

NO	Compound name	Chemical formula	M/Z	Trend
1	Betaine	$C_5H_{12}NO_2$	118.1543	↑
2	Hypoxanthine	$C_5H_4N_4O$	136.1115	↑
3	DL-threo-beta-Methylaspartic acid	$C_5H_9NO_4$	147.13	↑
4	L-carnitine	$C_7H_{16}NO_3$	162.2068	↑
5	7-Methoxychromone	$C_{10}H_9O_3$	177.17	↑
6	D-(+)-Pantothenic_acid	$C_9H_{17}NO_5$	219.235	—
7	Isobutyry-l-carnitine	$C_{11}H_{22}NO_4$	232.299	—
8	5′-Methylthioadenosine	$C_{11}H_{15}N_5O_3S$	297.334	↑
9	Cis-13-Docosenoic acid	$C_{22}H_{42}O_2$	338.5677	—
10	Di(5-nonyl) phthalate	$C_{28}H_{46}O_4$	446.662	—
11	SM(d18:0/16:1(9Z))	$C_{39}H_{79}N_2O_6P$	703.0281	↓
12	1,2-dipalmitoyl-sn-glycero-3-PC(DHPE)	$C_{37}H_{74}NO_8P$	691.972	↑
13	1-Stearoyl-2-linoleoyl-sn-glycero-3-phosphoethanolamine(1,2-dop/1,2-dielaidoyl)	$C_{41}H_{78}NO_8P$	744.034	—
14	2-Oleoyl-1-palmitoyl-sn-glycero-3-phosphocholine(POPC)	$C_{42}H_{82}NO_8P$	760.0761	↑
15	1,2-Dioleoyl PC(DOPC)	$C_{44}H_{84}NO_8P$	786.1134	↑
16	L-glutamine	$C_5H_{10}N_2O_3$	146.1445	↓
17	Orotic acid	$C_5H_4N_2O_4$	156.0963	↑
18	N-carbamoyl-L-Aspartic_acid	$C_5H_8N_2O_5$	176.1274	↓
19	2-Isopropylmalic acid	$C_7H_{12}O_5$	176.1672	—
20	Palmitic acid	$C_{16}H_{32}O_2$	256.424	—

2.3. Cell Activity Assay. DC2.4 cells were seeded into 96-well plates at a density of 3×10^5 cells/mL (100 μL for each well) and cultured for 24 h before discarding the medium. Complete culture medium containing different concentrations of LBP (0, 50, 100, 200 μg/mL) was added, respectively, and cultured for 24 h. The supernatant was discarded. 100 μL basal medium and 10 μL MTT solution (5 mg/mL) were added into each well and continued to culture for 4 h. 150 μL dimethyl sulfoxide were added to each well. Plates were shaken on a shaking table for 10 min to fully dissolve the crystals. The absorbance (Ab) at 450 nm and 630 nm of each well was measured using the microplate reader. The following formula was used to calculate cell activity: relative cell relative activity (%) = mean Ab (450 nm − 630 nm) value of polysaccharide group/mean Ab (450 nm − 630 nm) value of control group × 100%.

2.4. Cytokine Detection. DC2.4 cells were treated as previously mentioned in the present study. After supernatant was collected, the levels of IL-6, IL-12, and TNF-α were assayed by enzyme-linked immunosorbent assay (ELISA) kits according to user instructions.

2.5. Sample Processing for Metabolomic. DC2.4 cells were seeded into 6-well plates and treated with LBP concentration of 100 μg/mL. The cell culture medium was discarded. The plates were washed with precooled PBS for two times, and then washed with precooled normal saline (0.9% sodium chloride solution) for one time. The supernatant was completely discarded after each cleaning, and 1 mL ultrapure water was finally added. 100 μL sample was collected into a 1.5 mL centrifuge tube, 1000 μL extract (methanol: acetonitrile; water=2:2:1, V/V) was added, and mixed by shock. The samples were ultrasonically treated with ice water bath for 10 min, quick-frozen with liquid nitrogen for 1 min, repeated three times, and placed at -20°C for 1 h. After centrifugation at 13000 r and 4°C for 15 min, the supernatant was taken and dried with a nitrogen blower. 100 μL extract (acetonitrile: water=1:1, V/V) was added and the sample was shaken for 30 s. The sample was treated with ice water bath ultrasound for 10 min, and centrifuged at 13000 r under the condition of 4°C for 15 min. The supernatant was taken and prepared for testing.

2.6. UPLC-Q-TOF MS Conditions. Liquid phase conditions were shown as follows: UPLC BEH Amide Column (2.1 mm ×100 mm, 1.7 μm, Waters, USA); injection volume 5 μL; column temperature 55°C; mobile phase A-100% H_2O, B-100% ACN. Gradient elution conditions were as follows: at 0-1 min, 85% B; at 1-12 min, 65% B; at 12-12.1 min, 40% B; at 12.1-15 min, 40% B; at 15-15.1 min, 85% B; at 15.1-20 min, 85% B. The flow rate was 0.3 mL/min. Mass spectrometry conditions were as follows: UPLC-Q-TOF/MS (ESI) electrospray ionization source (X500R, AB SCIEX, USA); ion source temperature 600°C; ion source voltage -4500 V or 5500 V; curtain gas 20 psi, atomized gas and auxiliary gas both 60 psi. Multiple responses monitoring (MRM) was used for scanning.

2.7. Statistical Processing. UPLC-Q-TOF/MS technology was used to collect atlas information, and peak recognition, peak matching, peak retention time (RT) and quality (M/Z) data
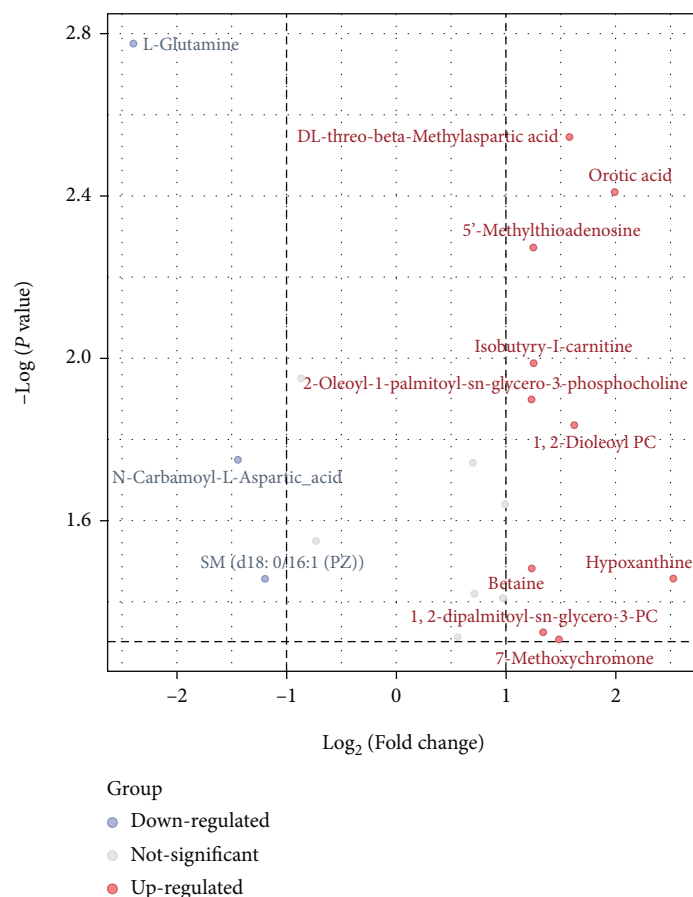
FIGURE 3: The volcanograms for identifying potential metabolites in LBP-induced DCs. The red dot is the upregulated metabolites with FC > 1.0 and $P < 0.05$, and the blue dot is the downregulated metabolites with FC> 1.0 and $P < 0.05$.

compared in XCMS and VGDB. The 3D data information was imported into R software. The clustering information and important variables were obtained by principal component analysis (PCA) and partial least squares discriminant analysis (PCA-DA). The PLS-DA model was used to calculate the VIP values of each variable in the samples. The differential metabolites between groups at different time points were screened according to VIP> 1.0. The data were normalized and log transformed, and the P value was calculated by t-test. When there was no biological duplication, only the fold change was calculated. Metabolites with log2 fold change ≥1 and $P ≤ 0.05$ were selected as the final differential metabolites. Qualitative analysis was performed on the primary and secondary spectrum data of mass spectrometry detection based on the Very Genome Database (VGDB), and material analysis was also performed by referring to other public mass spectrometry databases, including Mass-Bank, METLIN, HMDB, and MONA. Finally, metabolic pathway analysis was performed by MetaboAnalyst 5.0 (https://www.metaboanalyst.ca/).

3. Results

3.1. Effect of LBP on DC2.4 Cell Activity and Cytokine Secretion.
The effect of LBP on DC2.4 cell activity was measured by MTT assay. When the concentration of LBP was

50, 100 and 200 μg/mL, there was no significant inhibitory effect on DC2.4 cell (Figure 1(a)). On the contrary, LBP increased the cell activity significantly. Dendritic cells will secrete some cytokines during maturation, such as IL-6, IL-12, and TNF-α. In the present study, the results showed that LBP could promote the secretion of IL-6, IL-12, and TNF-α. In particular, LBP with the concentration of 100 μg/mL had the greatest promotion effect on the secretion of IL-6, IL-12, and TNF-α (Figure 1(b)–1(d)). Therefore, the concentration of LBP used in the subsequent metabolomics study was 100 μg/mL.

3.2. Method Stability Analysis.
The intracellular metabolites were analyzed by UPLC-Q-TOF-MS in both positive and negative ion modes in the present study. The total ions chromatogram is shown in Figure S1 and Table S1 and S2. The further detailed of global metabolic differences between the control group and LBP group were performed by multivariate statistical analysis. Firstly, principal component analysis (PCA) method and partial least-squares discriminant analysis (PLS-DA) model was used. The PCA scores plot (Figure 2(a)) showed good separation between the control group and LBP group, which provided a visual overview of the raw data without human influence. Then, PLS-DA was used to determine whether the model was reliable and over-
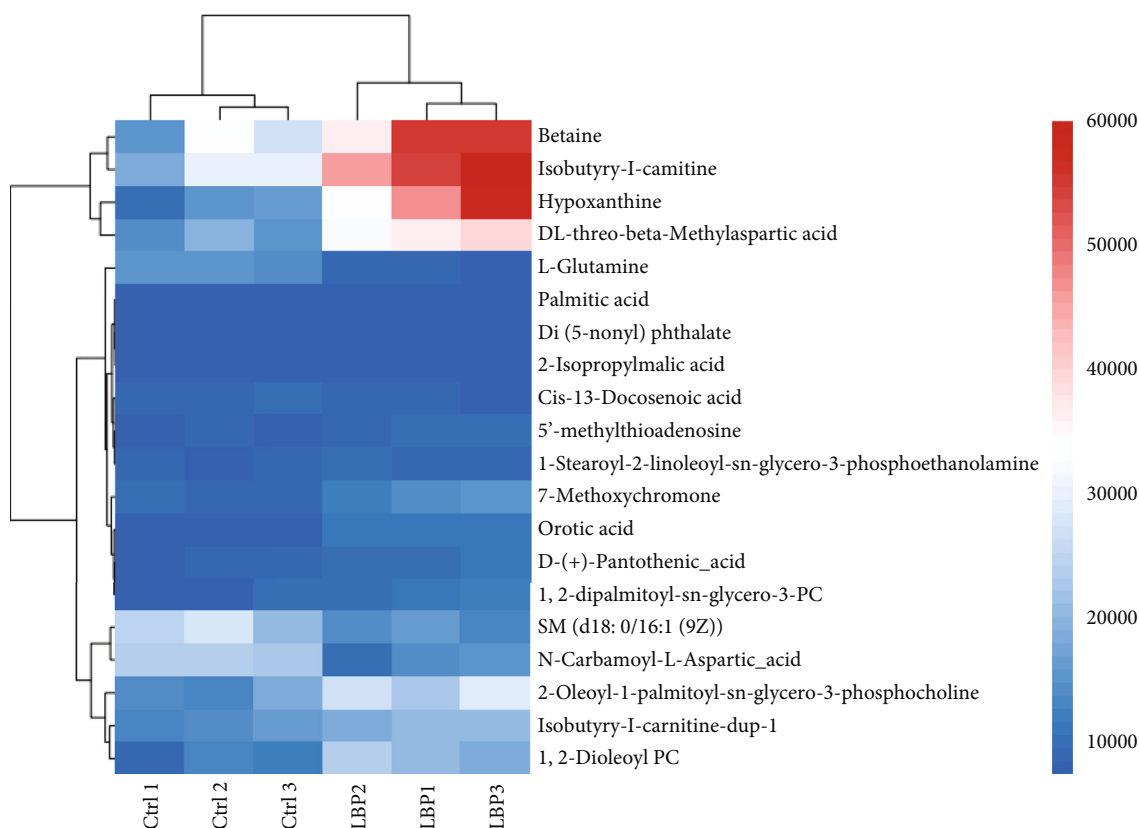
FIGURE 4: The heat map of the distribution of metabolites in LBP-induced DCs. Each small square represents a potential metabolite, and its color indicates the expression level of this metabolite. The greater the expression level, the darker the color (red represents upregulation, blue represents downregulation).

fitting according to R^2 and Q^2 in the results. The two groups of samples in the score chart of PLS-DA model (Figure 2(b)) could be distinguished, with R^2Y (cum) = 0.999 and Q^2 (cum) = 0.798. It is considered that the model was reliable and had good interpretation ability of original data without over-fitting. Furtherly, in order to improve the analytical ability and effectiveness of the PLS-DA model, orthogonal PLS-DA (OPLS-DA) model was established to obtain score graph (Figure 2(c)) and draw load graph (Figure 2(d)) according to VIP, both which showed that there were significant differences in potential biomarkers between control group and LBP group.

3.3. The Identification of Significantly Differential Metabolites.

For the samples of control group and LBP group, the metabolites with log2 fold change ≥1 and P value ≤0.05 were selected as the final differential metabolites. A total of 20 potential metabolites were screened from the raw pool as shown in Table 1. Among them, 10 metabolites were upregulated and 3 were downregulated. According to the variation of differential metabolites, volcanograms was further used to screen the differential metabolites as shown in Figure 3. The red dot is the upregulated metabolite with FC > 1.0 and $P < 0.05$, and the blue dot is the down-regulated metabolite with FC > 1.0 and $P < 0.05$. To help quickly and intuitively identify potential biomarkers that

vary widely and were statistically significant, the samples of each group were hierarchically clustered by using the expression of qualitative significant difference metabolites, and were represented by heat map (Figure 4). Each small square represents a potential metabolite, and its color varies with the concentration of metabolite. In this way, the changed of metabolite concentrations of LBP group versus control group could be found clearly, such as betaine, hypoxanthine, and DL threonine-beta-methylaspartic acid increased significantly in LBP group while L-glutamine decreased significantly. These results indicate that LBP has significant effects on dendritic cell metabolism.

3.4. KEGG Path Analysis.

To identify metabolic pathways affected by LBP in DCs, the significantly different metabolites which were found between LBP group and control group were analyzed using MetaboAnalyst. In the present study, the critical value of the influence value of metabolic pathway is set to 0.10. If it is higher than this threshold, this path will be selected as a potential target path. In this way, there were 28 metabolic pathways were found and summarized in Table 2. The top 25 metabolic pathways with $P < 0.6$ as shown in Figure 5, among which the top 5 metabolic pathways were aspartate metabolism ($P = 0.021$), pyrimidine metabolism ($P = 0.08$), phenylacetate metabolism ($P = 0.148$), methionine metabolism ($P = 0.173$) and fatty acid metabolism ($P = 0.173$).

Table 2: Analysis of cellular metabolic pathway based on metaboanalyst.

NO	Pathway name	Total	Expected	Hits	Raw p
1	Aspartate metabolism	35	0.615	3	0.021
2	Pyrimidine metabolism	59	1.04	3	0.08
3	Phenylacetate metabolism	9	0.158	1	0.148
4	Methionine metabolism	43	0.756	2	0.173
5	Fatty acid metabolism	43	0.756	2	0.173
6	Beta oxidation of very long chain fatty acids	17	0.299	1	0.262
7	Spermidine and Spermine biosynthesis	18	0.316	1	0.275
8	Pantothenate and CoA biosynthesis	21	0.369	1	0.313
9	Betaine metabolism	21	0.369	1	0.313
10	Carnitine synthesis	22	0.387	1	0.326
11	Glycerolipid metabolism	25	0.439	1	0.362
12	Oxidation of branched chain fatty acids	26	0.457	1	0.373
13	Purine metabolism	74	1.3	2	0.378
14	Mitochondrial Beta-oxidation of short chain saturated fatty acids	27	0.475	1	0.384
15	Mitochondrial Beta-oxidation of long chain saturated fatty acids	28	0.492	1	0.395
16	Phospholipid biosynthesis	29	0.51	1	0.406
17	Urea cycle	29	0.51	1	0.406
18	Ammonia recycling	32	0.562	1	0.438
19	Amino sugar metabolism	33	0.58	1	0.448
20	Beta-alanine metabolism	34	0.598	1	0.458
21	Fatty acid elongation in mitochondria	35	0.615	1	0.468
22	Fatty acid biosynthesis	35	0.615	1	0.468
23	Nicotinate and nicotinamide metabolism	37	0.65	1	0.487
24	Steroid biosynthesis	48	0.844	1	0.582
25	Glutamate metabolism	49	0.861	1	0.589
26	Warburg effect	58	1.02	1	0.653
27	Glycine and serine metabolism	59	1.04	1	0.66
28	Bile acid biosynthesis	65	1.14	1	0.696

4. Discussion

Current studies suggest that polysaccharides from traditional Chinese medicine may directly target DCs, activate and promote cell maturation, thereby affecting the immune response [15]. DCs are known to be the most effective and powerful antigen presenting cells in the body, and they are also the only full-time antigen presenting cells that can activate initial T cells [16, 17]. DCs release cytokines during activation and maturation, such as TNF-α, IL-6, IL-12, and chemokine ligands [18, 19]. Our study showed that LBP could significantly increase the activity of DC2.4 cells and stimulate the cells to secrete IL-6, TNF-α, and IL-12. Consistent with the previous studies [7–10], the results indicated that LBP promoted DCs maturation in the present study. However, we found it strange that the effect of LBP on TNF-α release of DCs showed little effect at the higher dose of 200 μg/mL. We speculate that this may be due to the existence of a negative feedback regulation mechanism on TNF-α.

To further investigate which metabolic pathways are involved in the promotion of DCs maturation by LBP, UPLC-Q-TOF-MS technology was used to determine DC2.4 cells metabolites in the present study and then the underlying metabolic pathways were analyzed. Our study showed that LBP could change 20 metabolites in DC2.4 cells, such as betaine, hypoxanthine, DL threonine-beta-methylaspartic acid, and L-glutamine. Among these metabolites, hypoxanthine, and L-glutamine had been shown to be involved in DCs activation and functional maturation [20]. The results suggest that LBP can affect DCs metabolism. Further pathway analysis suggested that these metabolites were involved in 28 metabolic pathways, such as aspartate metabolism, pyrimidine metabolism, phenylacetate metabolism, methionine metabolism, and fatty acid metabolism. Most of these pathways have been confirmed to be closely related to DCs activation, maturation, and T cell priming. For example, the aspartate metabolism is involved in mitochondrial respiration [21], and also plays a role in maturation and T cell priming of DCs by the IMP-S-AMP-MP cycle [20]. Fatty acid metabolism is involved in the glucose metabolism which is crucial for toll-like receptor (TLR)-induced activation of DCs [22], while inhibition of fatty acid metabolism could suppress DCs activation [23]. The inhibition of
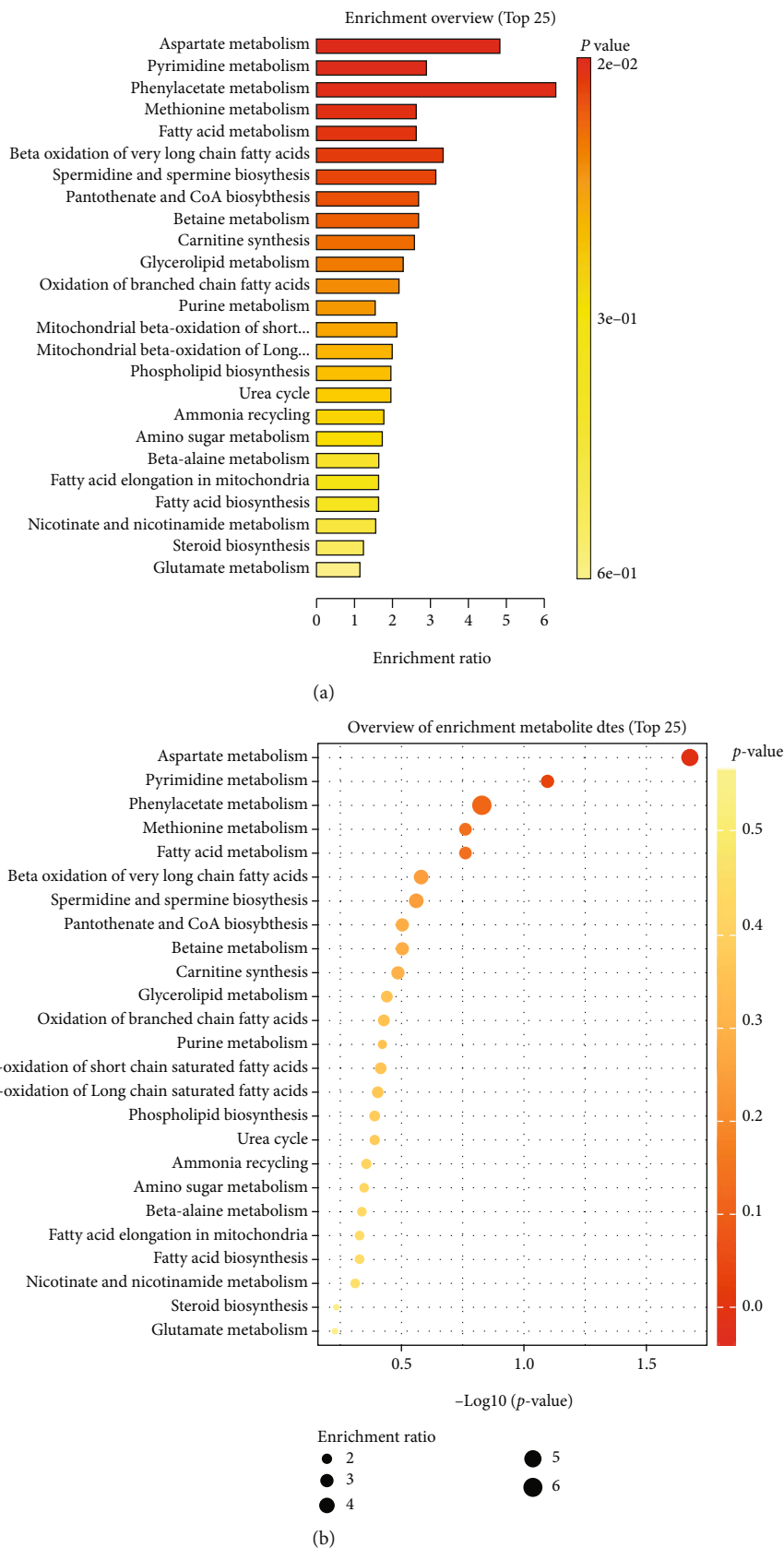
(a)

(b)

FIGURE 5: Metabolic pathways enrichment analysis of differential metabolites was conducted based on KEGG database. (a) Bar chart and (b) Bubble chart.

antigen-presenting activity of DCs resulting from UV irradiation of murine skin is restored by *in vitro* photorepair of cyclobutane pyrimidine dimers [24], this indicated that pyrimidine metabolism may involve in DCs metabolism.

In summary, the present study indicated that LBP promoted DCs maturation by the regulation of cell metabolism. Our previous study found that LBP could induce antitumor immune response and inhibit tumor growth in H22 tumor-bearing mice [11], so we speculated that these might be related to the regulation of DCs metabolism by LBP.

Data Availability

The underlying data supporting the results of our study were available on request. The corresponding author (Deng) is contacted to request the data.

Conflicts of Interest

The authors declare that they have no conflicts of interest.

Authors' Contributions

Baochen Zhang and Xiangliang Deng designed the study. Baochen Zhang, Li Liu, Xiuyun Li, Liang Han, and Zhongfeng Shi developed the methodology. Baochen Zhang, Li Liu, Xiuyun Li, and Enhui Wu acquired the data. Xiangliang Deng, Baochen Zhang, Kengyu Chen, and Zhongfeng Shi analyzed and interpreted the data. Baochen Zhang and Li Liu drafted the manuscript. Xiangliang Deng provided the financial support. Xiangliang Deng and Kengyu Chen revised the manuscript.

Acknowledgments

Supplementary Materials

Figure S1: the total ions chromatogram in negative ion and positive ion mode. Table Sl: the raw data of negative ion mode. Table S2: the raw data of positive ion mode. (Supplementary Materials). *(Supplementary Materials)*

References

[1] M. Cabeza-Cabrerizo, A. Cardoso, C. M. Minutti, M. Pereira da Costa, and C. Reis e Sousa, "Dendritic cells revisited," *Annual Review of Immunology*, vol. 39, no. 1, pp. 131–166, 2021.

[2] S. Ness, S. Lin, and J. R. Gordon, "Regulatory dendritic cells, T cell tolerance, and dendritic cell therapy for immunologic disease," *Frontiers in Immunology*, vol. 12, article 633436, 2021.

[3] A. Marolda, K. Hunniger, S. Bottcher et al., "Candida species-dependent release of IL-12 by dendritic cells induces different levels of NK cell Stimulation," *The Journal of Infectious Diseases*, vol. 221, no. 12, pp. 2060–2071, 2020.

[4] J. Tel, G. Schreibelt, S. P. Sittig et al., "Human plasmacytoid dendritic cells efficiently cross-present exogenous Ags to CD8$^+$ T cells despite lower ag uptake than myeloid dendritic cell subsets," *Blood*, vol. 121, no. 3, pp. 459–467, 2013.

[5] X. Peng, Y. He, J. Huang, Y. Tao, and S. Liu, "Metabolism of dendritic cells in tumor microenvironment: for immunotherapy," *Frontiers in Immunology*, vol. 12, article 613492, 2021.

[6] L. Zitvogel and G. Kroemer, "Targeting dendritic cell metabolism in cancer," *Nature Medicine*, vol. 16, no. 8, pp. 858-859, 2010.

[7] X. Duan, Y. Lan, X. Zhang et al., "Lycium barbarum polysaccharides promote maturity of murine dendritic cells through Toll-Like Receptor 4-Erk1/2-Blimp1 Signaling Pathway," *Journal of Immunology Research*, vol. 2020, Article ID 1751793, 15 pages, 2020.

[8] J. Zhu, Y. Zhang, Y. Shen, H. Zhou, and X. Yu, "Lycium barbarum polysaccharides induce toll-like receptor 2- and 4-mediated phenotypic and functional maturation of murine dendritic cells via activation of NF-κB," *Molecular Medicine Reports*, vol. 8, no. 4, pp. 1216–1220, 2013.

[9] R. Bo, Z. Liu, J. Zhang et al., "Mechanism of _Lycium barbarum_ polysaccharides liposomes on activating murine dendritic cells," *Carbohydrate Polymers*, vol. 205, pp. 540–549, 2019.

[10] W. Wang, M. Liu, Y. Wang et al., "_Lycium barbarum_ polysaccharide promotes maturation of dendritic cell via notch signaling and strengthens dendritic cell mediated T lymphocyte cytotoxicity on colon cancer cell CT26-WT," *Evidence-based Complementary and Alternative Medicine*, vol. 2018, Article ID 2305683, 10 pages, 2018.

[11] X. Deng, S. Luo, X. Luo et al., "Polysaccharides from Chinese herbal _Lycium barbarum_ Induced systemic and local immune responses in H22 tumor-bearing mice," *Journal of Immunology Research*, vol. 2018, Article ID 3431782, 12 pages, 2018.

[12] L. Guo, K. Chen, M. Sun et al., "Metabonomics: a useful tool to reveal underlying relationships between altered Chinese medicine syndromes and ultrafiltration in treatment of heart failure," *Chinese Journal of Integrative Medicine*, vol. 27, no. 4, pp. 259–264, 2021.

[13] X. Deng, X. Li, S. Luo, Y. Zheng, X. Luo, and L. Zhou, "Antitumor activity of *Lycium barbarum* polysaccharides with different molecular weights: an *in vitro* and *in vivo* study," *Food & Nutrition Research*, vol. 61, no. 1, article 1399770, 2017.

[14] X. Deng, Q. Liu, Y. Fu et al., "Effects of *Lycium barbarum* polysaccharides with different molecular weights on function of RAW264.7 macrophages," *Food and Agricultural Immunology.*, vol. 29, no. 1, pp. 808–820, 2018.

[15] S. Kikete, L. Luo, B. Jia, L. Wang, G. Ondieki, and Y. Bian, "Plant-derived polysaccharides activate dendritic cell-based anti-cancer immunity," *Cytotechnology*, vol. 70, no. 4, pp. 1097–1110, 2018.

[16] Y. Wang, Y. Xiang, V. W. Xin et al., "Dendritic cell biology and its role in tumor immunotherapy," *Journal of Hematology & Oncology*, vol. 13, no. 1, p. 107, 2020.

[17] A. Gardner, P. A. de Mingo, and B. Ruffell, "Dendritic cells and their role in immunotherapy," *Frontiers in Immunology*, vol. 11, p. 924, 2020.

[18] A. N. Wilkinson, K. Chang, R. D. Kuns et al., "IL-6 dysregulation originates in dendritic cells and mediates graft-versus-host disease via classical signaling," *Blood*, vol. 134, no. 23, pp. 2092–2106, 2019.

[19] T. C. Theoharides and P. Conti, "Mast cells to dendritic cells: Let IL-13 shut your IL-12 down," *The Journal of Allergy and Clinical Immunology*, vol. 147, no. 6, pp. 2073-2074, 2021.

[20] S. Saveljeva, G. W. Sewell, K. Ramshorn et al., "A purine metabolic checkpoint that prevents autoimmunity and autoinflammation," *Cell Metabolism*, vol. 34, no. 1, pp. 106–124.e10, 2022.

[21] L. B. Sullivan, D. Y. Gui, A. M. Hosios, L. N. Bush, E. Freinkman, and M. G. Vander Heiden, "Supporting aspartate biosynthesis is an essential function of respiration in proliferating cells," *Cell*, vol. 162, no. 3, pp. 552–563, 2015.

[22] E. J. Pearce and B. Everts, "Dendritic cell metabolism," *Nature Reviews. Immunology*, vol. 15, no. 1, pp. 18–29, 2015.

[23] C. C. Qiu, A. E. Atencio, and S. Gallucci, "Inhibition of fatty acid metabolism by etomoxir or TOFA suppresses murine dendritic cell activation without affecting viability," *Immunopharmacology and Immunotoxicology*, vol. 41, no. 3, pp. 361–369, 2019.

[24] A. A. Vink, A. M. Moodycliffe, V. Shreedhar et al., "The inhibition of antigen-presenting activity of dendritic cells resulting from UV irradiation of murine skin is restored by *in vitro* photorepair of cyclobutane pyrimidine dimers," *Proceedings of the National Academy of Sciences of the United States of America*, vol. 94, no. 10, pp. 5255–5260, 1997.